










## Research Article

# Synergistic Improvement of L-NAME Induced Hypertension Through the Combination of *Chuanxiong Rhizoma Hort.* and *Ganoderma lucidum Karst.*

Miaozhi Luo<sup>1</sup>, Fuling Wang<sup>1</sup>, Ruixin Wang<sup>1</sup>, Jinyi Wang<sup>1</sup>, Tong Lin<sup>1</sup>,  
Junyang Tan<sup>1</sup>, Huaiwei Liu<sup>1</sup>, Chenxue Li<sup>1</sup>, Bo Yang<sup>1</sup>, Jinchuan Zhao<sup>1,\*</sup>

<sup>1</sup>School of Pharmacy, Harbin University of Commerce, 150076 Harbin, Heilongjiang, China

\*Correspondence: [jc\\_alex\\_zhao@163.com](mailto:jc_alex_zhao@163.com) (Jinchuan Zhao)

Academic Editor: Mehmet Ozaslan

Submitted: 1 September 2025    Revised: 5 November 2025    Accepted: 12 November 2025    Published: 27 November 2025

## Abstract

**Background:** This study aimed to elucidate the therapeutic efficacy and underlying mechanisms of the combining of *Chuanxiong Rhizoma Hort.* (CX) and *Ganoderma lucidum Karst.* (GL) in treating hypertension (HTN) induced by chronic oxidative stress (OS). This research provides novel insights into the development of anti-hypertensive agents within the scope of medicine and food homologues, using network pharmacology and *in vivo* experimental validation. **Methods:** Active constituents and corresponding targets of CX and GL were respectively retrieved on the Traditional Chinese Medicine Systems Pharmacology (TCMSP) platform. Molecular docking was utilized to assess the binding efficacy between the constituents and core targets. Moreover, Kyoto Encyclopedia of Genes and Genomes (KEGG) pathway and Gene Ontology Biological Process (GOBP) enrichment analyses were performed against the core targets. The anti-hypertensive effects of the combination were validated in the N-Nitro-L-arginine methyl ester (L-NAME)-induced hypertensive rat model; meanwhile, the potential mechanism of action was investigated through indices assay and pathological examination. **Results:** A total of 6 and 14 core active constituents of CX and GL, respectively, were identified, along with 30 and 39 potential corresponding targets. The molecular docking established prostaglandin-endoperoxide synthase 2 (PTGS2) as the target with the highest binding affinity for treating both HTN and OS. The KEGG pathway analysis revealed the presence of the “estrogen signaling” and “vascular endothelial growth factor (VEGF) signaling” pathways. Additionally, the GOBP analysis showed significant enrichment in the terms “positive regulation of nitric oxide (NO) biosynthetic process” and “negative regulation of smooth muscle contraction”. These findings highlight the shared pathways between CX and GL in relation to HTN and OS. Moreover, the *in vivo* experiments validated that the combined CX and GL treatment contributed to significantly decreasing systolic blood pressure (SBP) and serum Ang-II levels, increasing aortic prostaglandin I<sub>2</sub> (PGI<sub>2</sub>) and total antioxidant capacity (T-AOC), reducing aortic vascular cell adhesion molecule-1 (VCAM-1), reactive nitrogen species (RNS), and heart index, and improving the aortic damage in a synergistic pattern in the L-NAME-induced hypertensive rat model. **Conclusion:** Administering the combination of CX and GL synergistically treated OS-induced HTN by improving vascular endothelial NO transduction, vasodilation, and anti-oxidative capacity, via co-regulation of the estrogen and VEGF signaling pathways. This finding provides a perspective for the development of novel therapeutic strategies in the treatment of HTN based on the dietary-medicinal properties of Chinese medicine in treatment of HTN.

**Keywords:** *Chuanxiong Rhizoma Hort.*; *Ganoderma lucidum Karst.*; hypertension; oxidative stress; network pharmacology; molecular docking

## 1. Introduction

Hypertension (HTN), a condition characterized by persistently elevated blood pressure (BP) against arterial walls, arises from intricate interactions between genetic predisposition, environmental factors, and lifestyle choices [1]. Globally, HTN affects approximately one-fifth of the population, with the majority of cases occurring in adults aged 30 to 79 years old. Annually, HTN leads to about 10 million deaths, with the incidence rising all the time [2]. Furthermore, HTN is closely associated with the development of cardiovascular diseases, including stroke, ischemic heart disease, and coronary heart disease [3]. HTN represents a significant global public health challenge [4], neces-

sitating the increase of public awareness, the improvement of management strategies, and the development of more effective and safer anti-hypertensive therapeutics.

Oxidative stress (OS) serves as a significant etiological factor in the pathogenesis of HTN. Under physiological conditions, the human body maintains a robust anti-oxidant defense system to effectively neutralize reactive oxygen species (ROS) and reactive nitrogen species (RNS) generated during cellular metabolism, thereby mitigating disease progression and senescence [5]. However, an imbalance ensues when the produced ROS and RNS surpasses the capacity of endogenous enzymatic and non-enzymatic antioxidants, leading to the accumulation of ROS and RNS, and



ultimately, the occurrence of OS [6–8]. In this situation, excessive oxidative intermediates are generated, which induce endothelial cell damage and vascular dysfunction, and trigger inflammatory and immune responses that adversely affect the cardiovascular system. Consequently, the heart, vasculature, brain, kidneys, and other target organs are impaired, thereby promoting the development of HTN [9]. N-Nitro-L-arginine methyl ester (L-NAME), a non-specific nitric oxide synthase (NOS) inhibitor, competitively binds to and inhibits endothelial NOS to diminish NO bioavailability and synthesis. This action precipitates vasoconstriction, endothelial dysfunction, and heightened OS, ultimately culminating in HTN. As a result, L-NAME is frequently employed in the establishment of experimental models to investigate HTN induced by chronic OS [10].

Despite advancements in anti-hypertensive pharmacotherapy, effective BP control remains suboptimal, largely due to limitations in drug availability and adverse effects. Furthermore, current clinical medicine lacks sustained HTN effects, leading to frequent rebound of HTN. To address these concerns, a subset of patients seeks complementary and alternative medicine, including traditional Chinese medicine (TCM), to identify treatments with potentially enhanced efficacy and reduced adverse effects [11]. TCM, with over 2000 years of clinical application, is extensively utilized in cardiovascular disease management [12]. In recent years, the treatment of cardiovascular diseases with TCM has been vigorously discussed [13]. Featuring multi-target, multi-component, and holistic regulatory effects, TCM not only reduces BP but also ameliorates HTN-related clinical symptoms, improves quality of life, controls risk factors, and protects target organs like the heart, brain, and kidneys from damage [14]. Considering the TCM principle of “food and medicine homology”, the incorporation of food-based TCM with anti-hypertensive properties into daily diets or health supplements could potentially address the medical challenges associated with anti-hypertensive drug therapy, alleviate strain on healthcare resources, and possibly offer preventive benefits for hypertension [15,16].

As typical TCM herbs documented in the Shennong Ben Cao Jing, *Chuanxiong Rhizoma Hort.* (CX) and *Ganoderma lucidum Karst.* (GL) have been used for thousands of years. The dried rhizome of the Apiaceae plant *Ligusticum chuanxiong Hort.*, is traditionally recognized for its pharmacological effects of promoting blood circulation, regulating breathing, dispelling wind, and alleviating pain. Many contemporary studies have validated that CX can be used for effectively treating atherosclerosis [17–19] and hypertension [20], among other cardiovascular pathologies. Nowadays, lots of classic prescriptions containing CX have been developed into proprietary Chinese medicines. For example, Dachuanxiong Koufuye and Fufang Chuanxiong Pill can enhance blood circulation and regulate hepatic function to alleviate wind-induced condi-

tions [21]. GL, the dried fruiting bodies of *Ganoderma lucidum Karst.* or *Ganoderma sinense*, is distinguished within the fungal kingdom for their notable medicinal properties, frequently applied in both pharmaceutical applications and dietary supplements [22]. The Compendium of Materia Medica, the first Chinese pharmacopoeia, records that in 1590 during the Ming Dynasty, GL has been attributed with therapeutic properties, such as tonifying the kidney, enhancing vital energy, strengthening cardiac function, increasing memory, and exhibiting anti-aging effects. Contemporary research indicates that GL demonstrates significant therapeutic potential in the management of HTN [23]. Since the anti-hypertensive effects of the combination are rarely explored, this study aims to investigate the synergistic anti-hypertensive effects and mechanism of the herbal pair through computational prediction and experimental validation, thereby providing a theoretical foundation for exploring its therapeutic potential in HTN management.

## 2. Materials and Methods

### 2.1 Network Pharmacology and Molecular Docking

#### 2.1.1 Screening of Active Constituents and Prediction of the Targets

On the Traditional Chinese Medicine Systems Pharmacology Database and Analysis Platform (TCMSP; <https://www.tcmsp-e.com/tcmsp.php>), the keywords “Chuanxiong” (CX in Chinese) and “Lingzhi” (GL in Chinese) were input with two critical indicators of clinical application for traditional Chinese medicine as the screening criteria [24]: Oral bioavailability (OB)  $\geq 30\%$  and drug-likeness (DL)  $\geq 0.18$ , to identify the potential bioactive components in CX and GL. Then the potential targets associated with the effective components of CX and GL were analyzed, with “validated targets” as the selection criterion. The Uniprot database (<https://www.uniprot.org/>) was then utilized to convert the target proteins of each bioactive component into corresponding gene names, with deduplication.

Utilizing the databases Genecards (<https://www.genecards.org/>), TTD (<https://db.idrblab.net/ttd/>), and OMIM (<https://www.omim.org/>), a comprehensive search was conducted using the keywords “hypertension” and “oxidative stress” to identify all pertinent targets HTN and OS, respectively. The resultant datasets were then subjected to an intersection operation, with the redundant entries eliminated.

#### 2.1.2 Network Construction and Identification of Core Targets

On the BioLadder bioinformatics platform (<https://www.bioladder.cn/web/#/pro/cloud>), the intersection of active components and the predicted targets for CX and GL associated with HTN or OS was determined, respectively. A Venn diagram was in turn generated. A network diagram was



constructed using the software Cytoscape (version 3.10.2, Institute for Systems Biology, Seattle, WA, USA).

The identified intersection targets were subsequently imported into the STRING 12.0 platform (<https://string-db.org/>), with “Homo sapiens” designated as the selected organism. The “Minimum Required Interaction Score” was set as “ $\geq 0.4$ ”. Nodes with disconnected networks were hidden. A protein–protein interaction (PPI) network was constructed and exported as a “.tsv” file. Utilizing the Cytohubba plugin within Cytoscape, the core targets were filtered based on the top-ranked degree values.

### 2.1.3 Molecular Docking

According to the degree values, the top five key targets were selected for the docking analysis, following the screening of the primary active components of CX and GL with the targets identified through PPI analysis. Initially, the 3D structures of the relevant genes were retrieved from the Uniprot and PDB (<http://www.rcsb.org/>) databases. Subsequently, crystallographic water molecules and other small molecules were removed from the receptor protein structures using software PyMOL (version 3.0.3, DeLano Scientific LLC, San Carlos, CA, USA), thereby establishing the receptor molecules for subsequent analysis. Subsequently, the “mol2” format of the primary constituents of CX and GL, serving as ligands, was obtained from the TCMSP database. The molecular docking was performed using software AutoDockTools (version 1.5.7, Olson Laboratory of Scripps Institute, San Diego, CA, USA), and the “optimal docking pose” was selected as the result of the molecular docking analysis. The binding energy reflects the stability of the interaction between the active component and the key target protein; a lower binding energy indicates a more stable docking conformation. The results were visualized using PyMOL software.

### 2.1.4 GO Function and KEGG Pathway Enrichment

All the identified core targets were imported into the DAVID platform (<https://davidbioinformatics.nih.gov/home.jsp>). The Kyoto Encyclopedia of Genes and Genomes (KEGG) pathway enrichment analyses and GO biological process (GOBP) enrichment analysis of the targets were performed under a *p*-value threshold of less than 0.05. The resultant data were visualized to facilitate the prediction of potential functional pathways.

## 2.2 Experimental Verification

### 2.2.1 Experimental Animals

Male 6-week-old Sprague-Dawley rats were purchased from Changsheng Biotechnology Co., Ltd., Benxi, Liaoning, China. Feeding conditions: Ad libitum food and water intake, artificial light illumination (12 h light/dark cycle), 24 °C temperature, 40%–60% relative humidity and adaptive feeding for 7 days. Laboratory animal permission license number: SYXK(Hei)2024-012. The research pro-

cedure was approved by the Animal Research Ethics Committee of Harbin University of Commerce (Approval No.: HSDYXY-2024066).

### 2.2.2 Experimental Devices and Reagents

**2.2.2.1 Experimental Devices.** Non-invasive blood pressure measurement system for rats (Equipment No. KW2022112427, Calvin Biotechnology Co., Ltd., Nanjing, Jiangsu, China); ST-360 microplate reader (Equipment No. 20212220416, Kehua Experimental System Co., Ltd., Shanghai, China); LE204E/02 electronic balance (Equipment No. BSA224S, Sartorius Instrument System Engineering Co., Ltd., Beijing, China); 2135 rotary microtome (LEICA Biosystem, Nussloch, Germany).

**2.2.2.2 The Herbal Products and Preparation.** The raw *Chuanxiong Rhizoma Hort.* (CX) and *Ganoderma lucidum* Karst. (GL) were purchased from Nanjing Tongrentang, the specialty store for Chinese herbal medicinal materials (both harvested at Bozhou in Anhui Province, China, in August. Lot No.: 6124442351 and 5917441916).

The quality control process was carried out referring to the Chinese Pharmacopoeia (Edition 2020) [21]. The products were both authenticated as the genuine products in the premier quality by Prof. Qu Zhongyuan from school of Pharmacy, Harbin University of Commerce. The quantitative analysis revealed that the ferulic acid content in CX is 0.13% in average, which is higher than the criterion 0.10%; the total content of triterpenoid and sterols in GL was measured as 0.97% in average, which is higher than the criterion 0.50%. Both of the herbal products comply with the criterion outlined in the 2020 Chinese Pharmacopoeia (see **Supplementary Material 1** for details).

The authenticated products were grinded into ultrafine powder, dissolved in distilled water and thoroughly mixed right before the administration. The gavage volume for the mixed solution of the products was 1.0 mL/100 g (body weight).

**2.2.2.3 Experimental Reagents.** L-NAME (Dalian Meilun Biotechnology Co., purity >98%), captopril (Dalian Meilun Biotechnology Co., purity >98%), sodium pentobarbital (Beijing Chemical Reagent Research Institute Co., Ltd., purity >98%), and distilled water.

HE (hematoxylin-eosin staining) reagents: 10% neutral buffered formalin (NBF), Harris hematoxylin, alcohol-soluble eosin Y, 1% acid alcohol, 95% ethanol, xylene, Scott's tap water substitute, neutral balsam.

Reagent kits: rat Angiotensin II (AngII) ELISA research kit (JM-01618R1, Jingmei Biotechnology Co., Ltd., Yancheng, Jiangsu, China), rat prostaglandin I<sub>2</sub> (PGI<sub>2</sub>) ELISA research kit (JM-02114R2, Jingmei Biotechnology Co., Ltd., Yancheng, Jiangsu, China), rat vascular cell adhesion molecule-1 (VCAM-1) ELISA research kit (JM-10755R2, Jingmei Biotechnology Co., Ltd., Yancheng,

Jiangsu, China), total antioxidant capacity (T-AOC) assay research kit (FRAP method) (A015-3-1. Jiancheng Bioengineering Institute, Nanjing, Jiangsu, China), and reactive nitrogen species (RNS) assay research kit (Microwell plate method) (A013-2-1. Jiancheng Bioengineering Institute, Nanjing, Jiangsu, China).

### 2.2.3 Hypertension Model Preparation

SD rats were randomly divided into the blank control group and model induction group. The model induction group was given 6 mg/kg L-NAME dissolved in distilled water by gavage every day, while the blank control group was given the same volume of distilled water. Four weeks later, rats with a systolic blood pressure (SBP) increase of more than 20 mmHg were selected as models for the next experiments.

### 2.2.4 Drug Administration Experiment

**2.2.4.1 Effective Dosage of CX and GL Determination.** The modelled hypertensive rats were randomly divided into the following administration groups: CX lower-, medium- and higher- dosage groups (CX-L: 50 mg/kg, CX-M: 100 mg/kg, CX-H: 300 mg/kg) and GL lower-, medium- and higher- dosage groups (GL-L: 50 mg/kg, GL-M: 100 mg/kg, GL-H: 300 mg/kg), while the blank group and model group were given an equal volume of solvent by gavage for 3 weeks. The administration of intragastric L-NAME was continued during that of the drugs, with a 12-hour interval. SBP of each group was measured once a week during the administration.

**2.2.4.2 Combination of CX and GL Administration.** The modelled hypertensive rats were randomly divided into the following administration groups: CX group (CX, 100 mg/kg), GL group (GL, 100 mg/kg), CX and GL combination group (Combo, 100 mg/kg for each), Captopril group (Capt, 10 mg/kg), and the blank group and model group were given an equal volume of solvent by gavage for 3 weeks. The administration of intragastric L-NAME was continued during that of the drugs, with a 12-hour interval. SBP of each group was measured once a week during the administration, and the combination index (CI) value [25] was calculated by the Chou-Talalay method [26] to analyze the synergistic effect.

### 2.2.5 Indicators and Pathological Detection

The rats were weighed and i.p. anesthetized with 42 mg/kg 3% sodium pentobarbital after 16 h fasting following the last administration. The dosage was strictly calculated based on the animal's body weight, with the volume of 1.5 mL/kg. During the administration, the warmth was maintained. Death was confirmed by absent respiration and no toe-pinch response. The serum, heart and thoracic aorta were then carefully collected. The concentration of serum AngII and aortic PGI<sub>2</sub>, VCAM-1, RNS, T-AOC were de-

tected using the ELISA kits. The heart was weighed to calculate the heart index.

The same part of the thoracic aortas for each individual was prepared for the HE staining, following a regular procedure: 10% NBF fixation for over 24 hours → dehydration (sequential immersion in graded ethanol solutions) → clearing (xylene immersion) → wax immersion → embedding → sectioning → slide baking → dewaxing → Harris hematoxylin staining (10 min) → differentiation (1% acid alcohol for 3 s) and bluing (Scott's bluing solution for 5–10 min) → eosin staining (1–3 min in eosin solution) → clearing with xylene → mounting with neutral balsam.

### 2.2.6 Statistical Analysis

All data were analyzed and processed using the software IBM SPSS Statistics (version 26.0. Chicago, IL, USA). The results were expressed as “mean ± standard deviation ( $\bar{x} \pm s$ )”. LSD one-way analysis of variance was used for comparison among multiple groups. A  $p$ -value < 0.05 was considered statistically significant. The software Origin (version 2024. OriginLab Company, Northampton, MA, USA) was used for the plotting.

## 3. Results

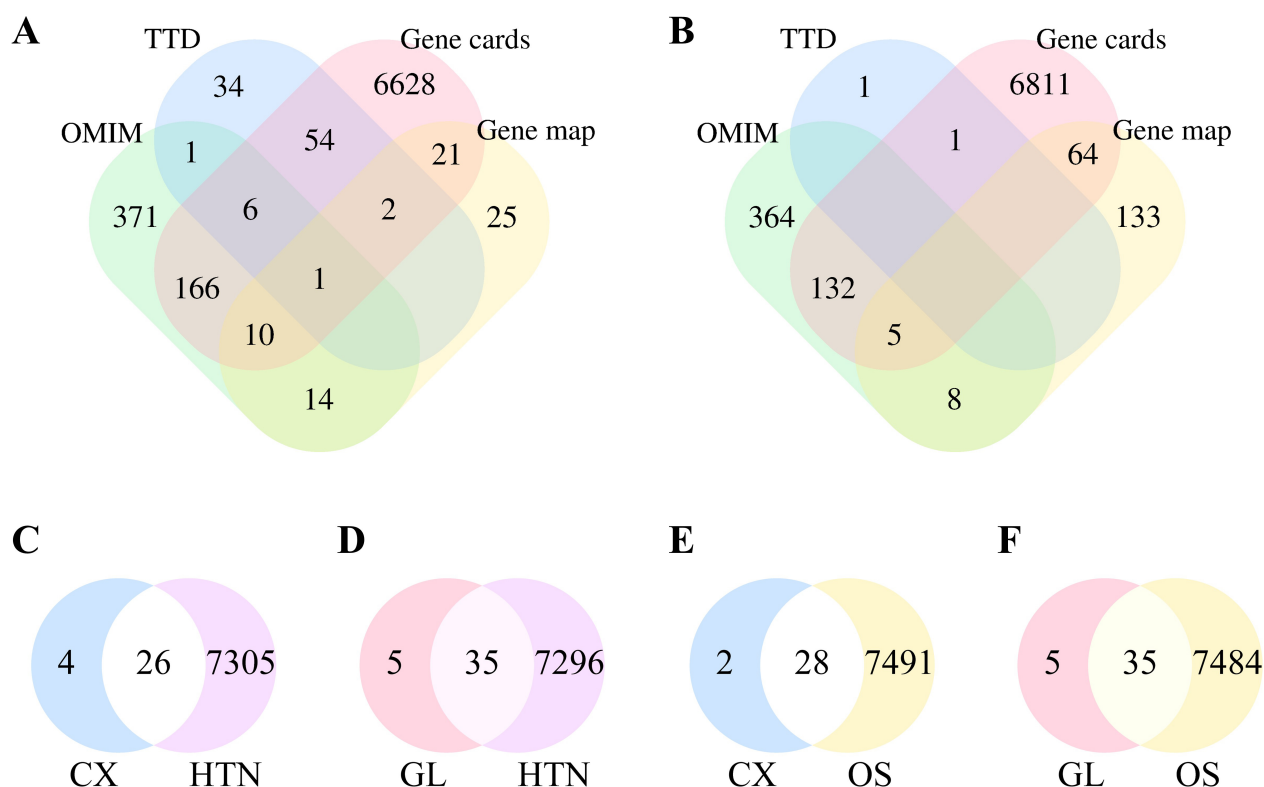
### 3.1 Network Pharmacology and Molecular Docking

#### 3.1.1 Screening of Active Constituents and Target Prediction for CX and GL

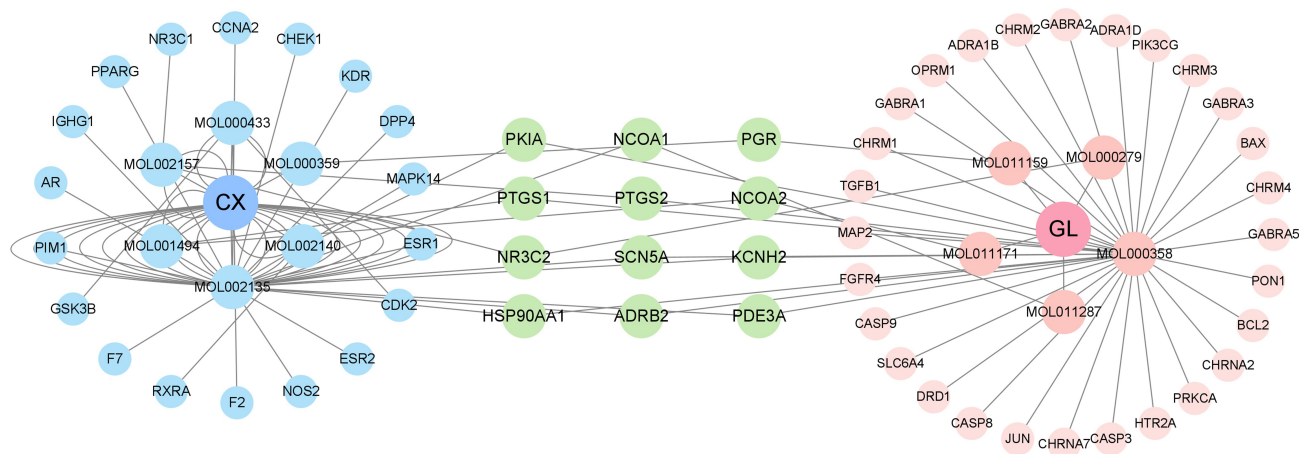
**3.1.1.1 Screening of Active Constituents for CX and GL.** On the TCMSP platform, 189 active components of CX and 242 active components of GL were retrieved. Using “OB ≥ 30%” and “DL ≥ 0.18” as the screening criteria, 7 major components of CX and 61 major active components of GL were obtained. Among them, 6 components of CX and 14 components of GL had corresponding protein targets (see **Supplementary Material 2-Tables 1,2**).

**3.1.1.2 Predicted Targets of CX and GL.** On the TCMSP platform, 30 and 39 potential targets were identified associated with the active components of CX and GL (see **Supplementary Material 2-Tables 3,4**), respectively. 57 related targets for the combined use of CX and GL were obtained (see **Supplementary Material 2-Table 5**).

**3.1.1.3 Analysis of Targets Related to HTN and OS.** Adopting the median value once in the GeneCards database, 6840 and 7013 protein targets were identified associated with HTN and OS, respectively. 100 HTN-related and 2 OS-related protein targets were yielded in the TTD database. 812 HTN-related and 811 OS-related protein targets were retrieved from the OMIM database. 73 HTN-related and 210 OS-related protein targets were identified in the Gene Map database. By summary of the protein targets obtained from each database and the redundancies elimination, a total of 7331 unique HTN-related protein targets (see



**Fig. 1. Results of targets analysis presented.** (A) Number of targets associated with HTN. (B) Number of targets associated with OS. (C) Intersection of targets between CX and HTN. (D) Intersection of targets between GL and HTN. (E) Intersection of targets between CX and OS. (F) Intersection of targets between GL and OS. HTN, hypertension; CX, *Chuanxiong Rhizoma Hort.*; GL, *Ganoderma lucidum Karst.*; OS, oxidative stress.



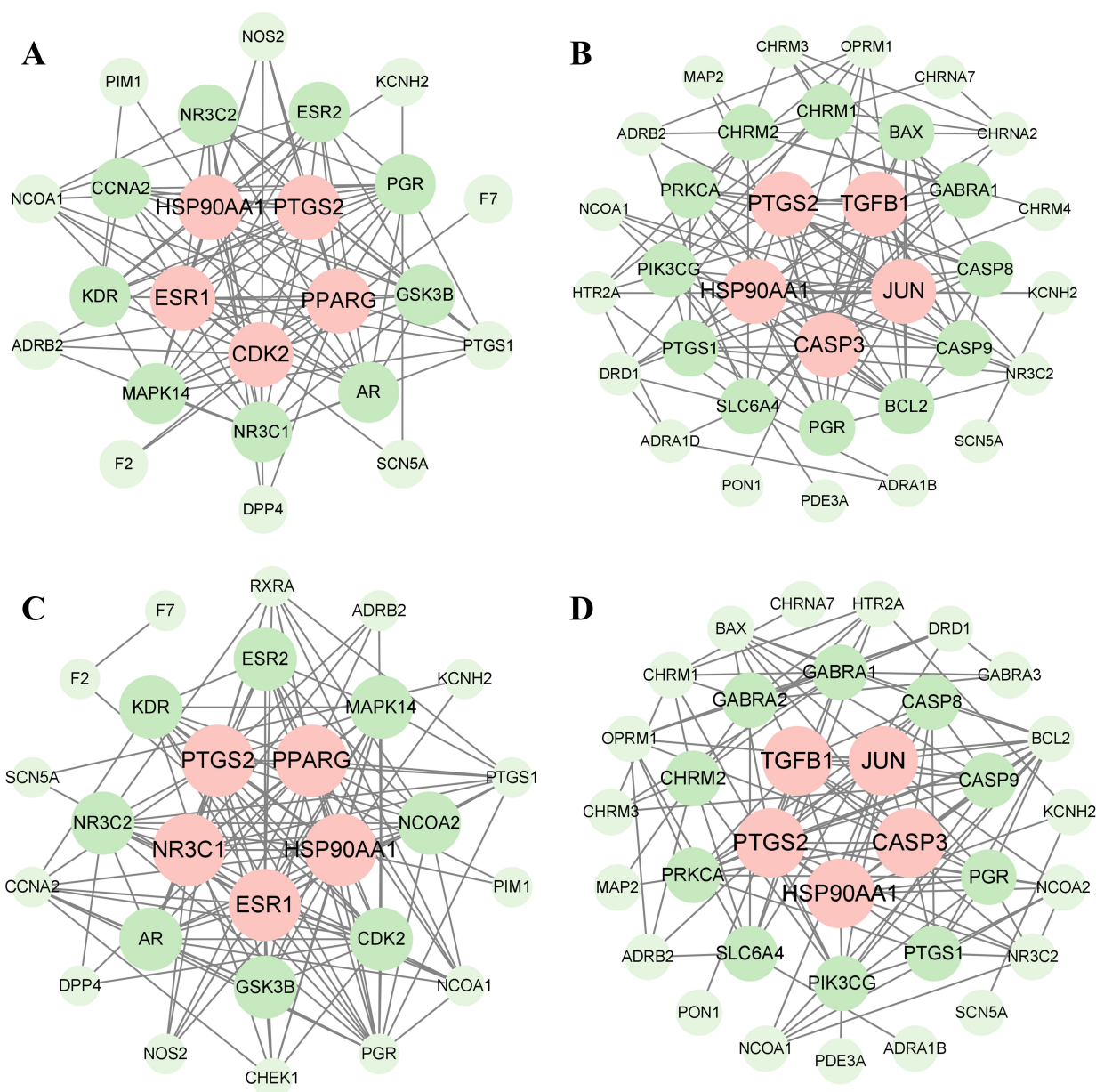
**Fig. 2. The active components - targets network in combination of CX and GL.** The middle section represented the 12 common target genes of the active components of both (see **Supplementary Material 2-Tables 1–5** for more details).

Fig. 1A) and 7519 unique OS-related protein targets (see Fig. 1B) were obtained presented by the Venn diagram.

### 3.1.2 Network Construction and Identification of Core Targets

**3.1.2.1 Network Construction.** The intersection of the action targets of CX and GL combined with HTN and OS disease was retrieved based on the results above (see **Supple-**

**mentary Material 2-Table 6**). 26 mutual targets were collected between the main active components of CX and HTN (see Fig. 1C), 35 ones were collected between the main active components of GL and HTN (Fig. 1D), 28 ones were collected between the main active components of CX and OS (Fig. 1E), 35 ones were collected between the main active components of GL and OS (Fig. 1F).



**Fig. 3. Results of core targets identification.** (A) PPI network of CX and HTN-related proteins. (B) PPI network of GL and HTN-related proteins. (C) PPI network of CX and OS-related proteins. (D) PPI network of GL and OS-related proteins. The core targets are aligned in the center and marked as pink. PPI, protein–protein interaction.

The “active components–targets” network was shown in Fig. 2. The left side illustrated the six active components of CX and their corresponding target genes; the right side illustrated the five active components of GL and their corresponding target genes; the middle section represented the 12 common target genes of the active components of both.

**3.1.2.2 Core Targets Identification.** PPI networks were constructed to identify core targets of CX and GL, as well as their intersections with HTN and OS (see Fig. 3A–D).

### 3.1.3 Molecular Docking

Molecular docking was performed for the top 5 key targets and active components selected from the PPI networks based on degree values (see **Supplementary Material 2-Table 7**). A total of 100 ligand-receptor docking results were obtained (see Fig. 4A,B). The pairs perillyrin (from CX) – prostaglandin-endoperoxide synthase 2 (PTGS2) and lucidone A (from GL) – PTGS2 were docked with the lowest binding energy (–9.8 kcal/mol and –9.2 kcal/mol) respectively, for both HTN and OS (see Fig. 4A,B and Fig. 5A,B).



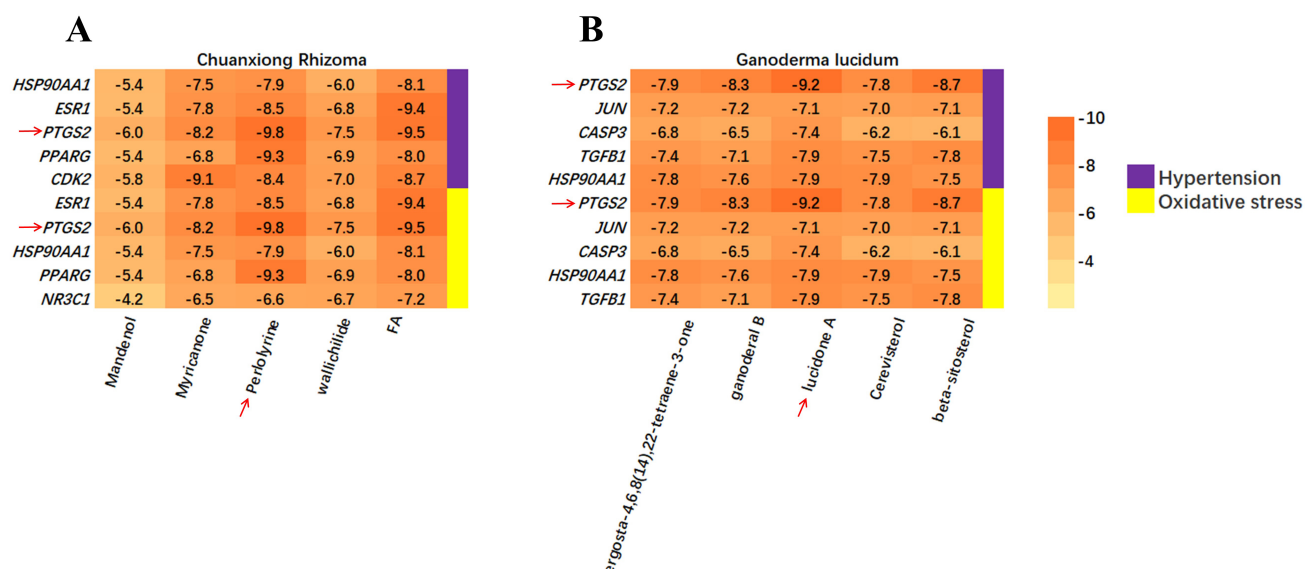


**Fig. 4. Calculation of the binding energy.** (A) Binding energy between core targets and constituents of CX. The red arrows indicate PTGS2 and perlolyrine. (B) Binding energy between core targets and constituents of GL. The red arrows indicate PTGS2 and lucidone A. PTGS2, prostaglandin-endoperoxide synthase 2.

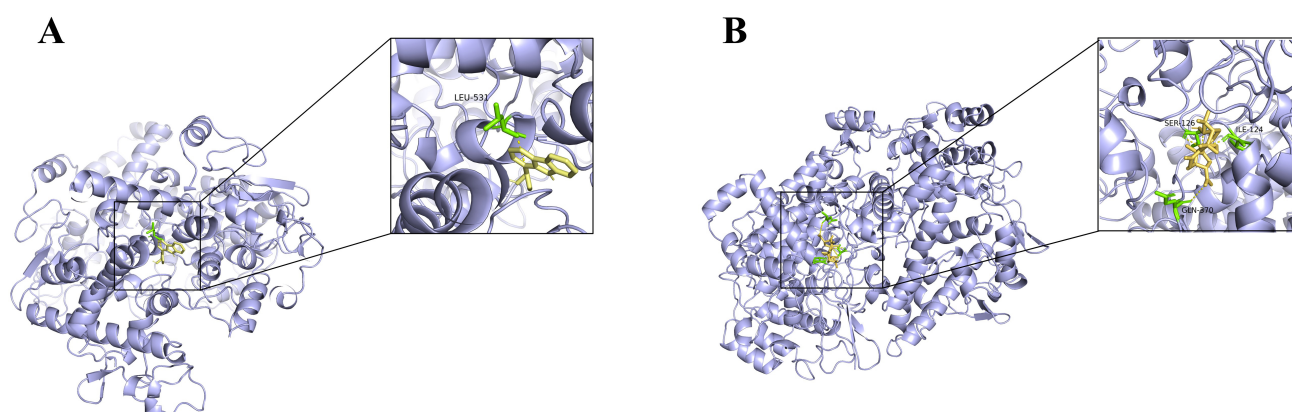


**Fig. 5. Analog images of docking.** (A) Analog image of docking between Perlolyrine (from CX) and PTGS2. (B) Analog image of docking between Lucidone A (from GL) and PTGS2.

### 3.1.4 KEGG Pathway and GOBP Enrichment Analysis

The KEGG enrichment analysis was performed on the identified core targets of CX and GL, respectively, associated with HTN or OS. The top 30 signaling pathways were selected for each by sorting the *p* values in ascending order, to form the bubble charts (see Fig. 6A–D). The mutual KEGG pathways “Estrogen signaling pathway” and “VEGF (vascular endothelial growth factor) signaling pathway” triggered by CX and GL, which were highly associated with HTN and in endothelial Nitric Oxide Synthase (eNOS) was involved in, were screened out of the 12 mutual ones between 12 HTN - related and 15 OS - related terms (see **Supplementary Material 2-Tables 8,9**); the core targets and corresponding biological functions involved in the pathway were illustrated as in Fig. 7.

The GOBP enrichment analysis was performed on the targets as well. The number of significantly enriched GOBPs was shown in Fig. 8A,B. The mutual significantly enriched GOBP terms between CX and GL “positive regulation of nitric oxide (NO) biosynthetic process” and “negative regulation of smooth muscle contraction”, which were the most highly related to hypertensive pathology given prior knowledge, were screened out of the 9 mutual ones between 19 HTN-related and 10 OS-related terms (see **Supplementary Material 2-Tables 10,11**).

The constructed network of components - targets - pathways and biological processes indicated that the combination of CX and GL could synergistically improve the HTN induced by NO depletion, by regulating the vascular NO signaling conduction and smooth muscle contraction via the Estrogen and VEGF signaling pathway in common.

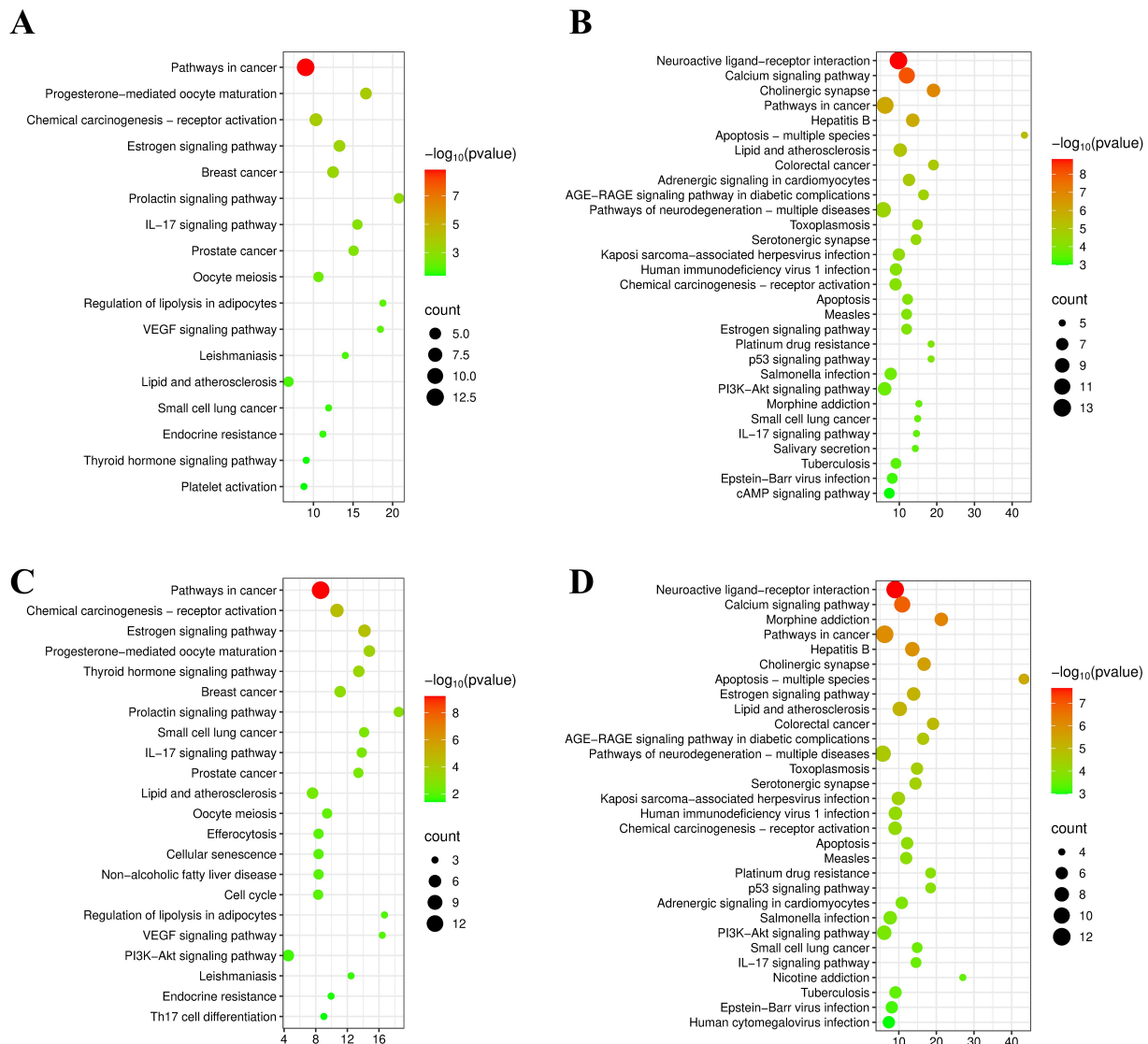


**Fig. 6. Enrichment analysis results.** (A) Enriched KEGG pathways for CX associated with HTN. (B) Enriched KEGG pathways for GL associated with HTN. (C) Enriched KEGG pathways for CX associated with OS. (D) Enriched KEGG pathways for GL associated with OS. KEGG, Kyoto Encyclopedia of Genes and Genomes.

### 3.2 Experimental Results

#### 3.2.1 Indices Measurement

The SBP of both CX and GL groups significantly decreased compared with that of the model group after three-week administration (see Fig. 9), indicating that the dosing range of 50–300 mg/kg exerted a significant anti-hypertensive effect on the L-NAME induced hypertensive rat model. The medium dosage (100 mg/kg) for both was applied in the experiments on the combination.

The SBP of the Combo group exhibited constant significant decrease compared with that of the model group during the three-week administration (see Fig. 10A). The CI values were all less than 1 at different time points (0.506

for week 1, 0.641 for week 2, 0.880 for week 3), demonstrating synergistic anti-hypertensive effects between CX and GL. The concentration of serum AngII of all administration groups was significantly lower than that of the model group ( $p < 0.001$ , as seen in Fig. 10B), in accordance with the BP measurements.

The index measurements revealed that, compared with the model group, the aortic expressions of PGI2, T-AOC, VCAM-1 and RNS and the value of heart index were all significantly different for the Combo group (see Fig. 10C–G). By contrast, those indices of the Combo group all performed more remarkably than those of the CX, GL or Capt group. Specifically, the aortic expressions of PGI2,

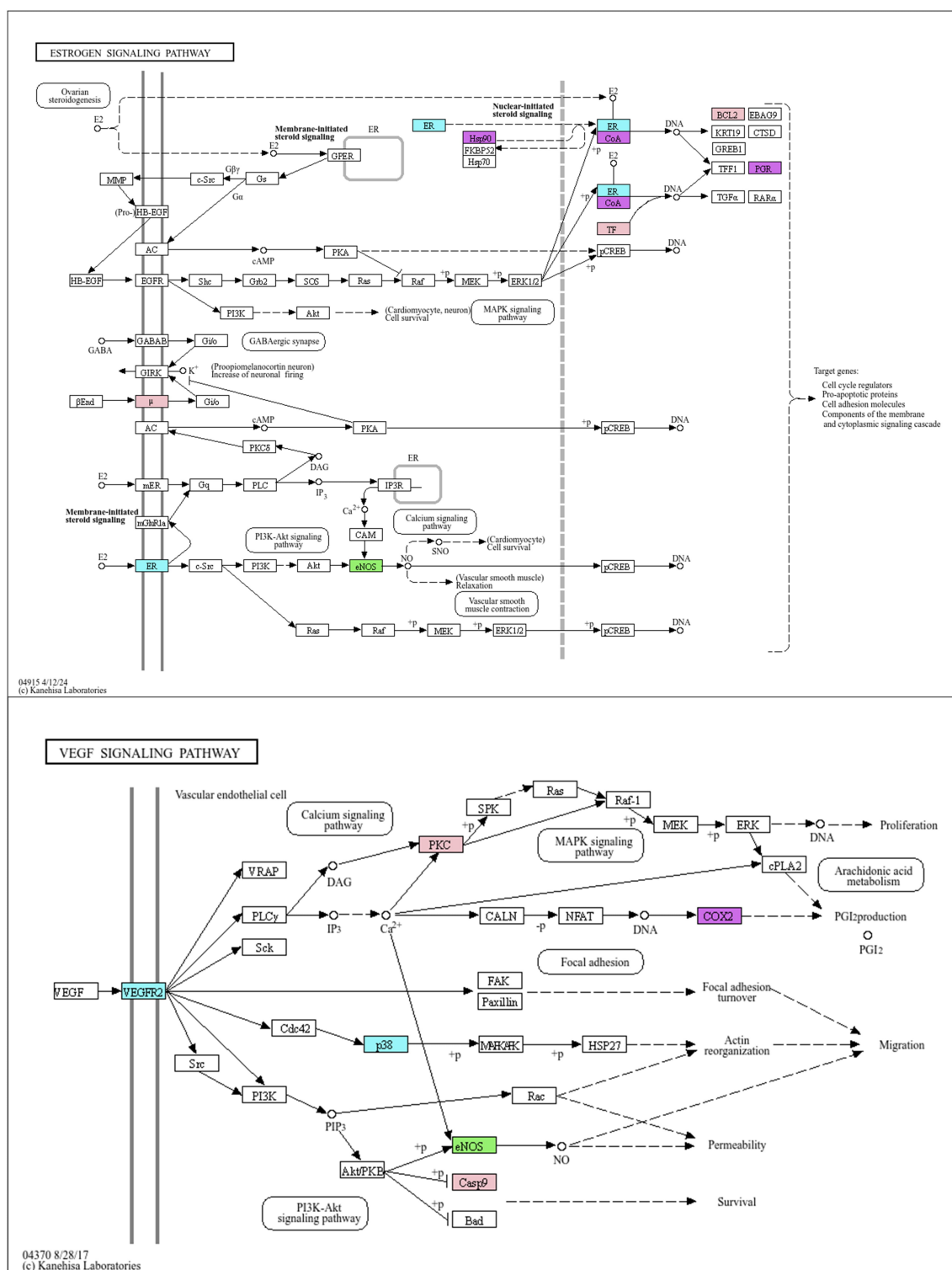


**Fig. 7. Mutual enriched KEGG pathways triggered by CX and GL: Estrogen signaling pathway and VEGF signaling pathway.** Target of L-NAME (green): eNOS; targets of CX (blue): ESR (ESR1 and ESR2), VEGFR2 (or KDR), *p38* (or *MAPK14*); targets of GL (pink):  $\mu$  (OPRM1), *TF* (transcription factor: *JUN*), *BCL2*, *PKC* (or *PRKCA*), *Casp9* (*CASP9*); mutual target of CX and GL (purple): *CoA* (*NCOA1*), *Hsp90* (*HSP90AA1*), *PGR*, *COX2* (or *PTGS2*). VEGF, vascular endothelial growth factor; L-NAME, N-Nitro-L-arginine methyl ester; eNOS, endothelial Nitric Oxide Synthase; VEGFR2 (KDR), Vascular Endothelial Growth Factor Receptor 2; *p38* (or *MAPK14*), mitogen-activated protein kinase;  $\mu$  (OPRM1), mu-1 opioid receptor; *TF* (*JUN*), Jun Proto-Oncogene; *BCL2*, Apoptosis regulator Bcl-2; *PKC* (*PRKCA*), Protein kinase C alpha type; *Casp9* (*CASP9*), Caspase-9; *CoA* (*NCOA1*), Nuclear receptor coactivator 1; *Hsp90* (*HSP90AA1*), Heat shock protein HSP 90-alpha; *PGR*, Progesterone receptor; *COX2*, Cyclooxygenase-2.



**Fig. 8. Number of the enriched GOBP terms.** (A) Number of enriched GOBPs for core targets of CX and GL associated with HTN. (B) Number of enriched GOBPs for core targets of CX and GL associated with OS. GOBP, Gene Ontology Biological Process.

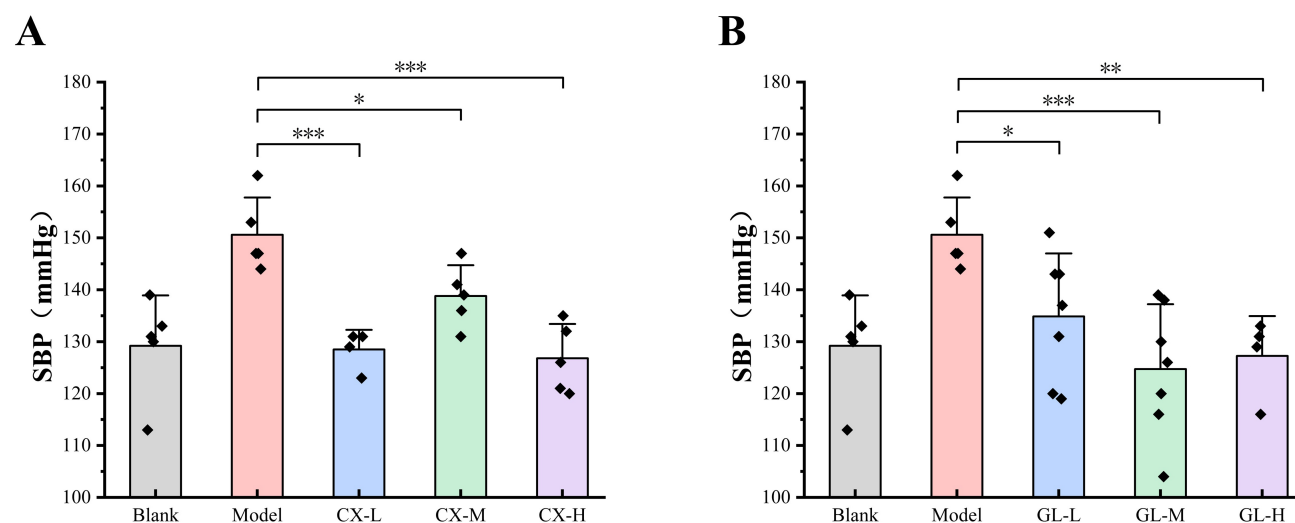


**Fig. 9. Effective dosage of single drug administration.** (A) SBP of CX groups after three-week administration. (B) SBP of GL groups after three-week administration. Lower dosage (L): 50 mg/kg; Medium dosage (M): 100 mg/kg; Higher dosage (H): 300 mg/kg. Compared with the model group, \* $p < 0.05$ , \*\* $p < 0.01$ , \*\*\* $p < 0.001$ .  $n = 4-7$ . SBP, systolic blood pressure.

VCAM-1 and RNS and the heart index showed no significant difference with those of the model when CX or GL was administered alone. In addition, the body weight of the Capt group significantly decreased compared with that of the model group ( $p < 0.05$ ), while none of the other administration groups showed such significant difference (see Fig. 10H).

### 3.2.2 Pathological Detection

Fig. 11 presents the results of the HE staining of the thoracic aorta. The intact endothelial structure and vessel tissue were constantly observed in the blank group, with normal morphology and clear boundaries of smooth muscle cells in the tunica media, and abundant, regularly arranged collagen fibers in the outer layer. In the model group, extensive loss of endothelial structure (black arrows) was identified in the vessel tissue, while hydropic degeneration of smooth muscle cells in the tunica media was evident, with cell swelling and pale staining of the cytoplasm (red arrows). Both the CX group and the GL group showed a small amount of endothelial structure loss in the vessel tissue, and

a small amount of hydropic degeneration of smooth muscle cells in the tunica media, with pale staining of the cytoplasm. In the Combo group, the vascular endothelial structure exhibited minor focal disruptions. Vascular smooth muscle cells maintained normal morphology, with better overall structural integrity compared with the model group. No significant infiltration of inflammatory cells, edema, or aberrant proliferation of fibrous tissue was observed in the Combo group, indicating a preserved vascular architecture. The results of the Capt were similar to those of the Combo group.

### 3.3 Summary of Results

The workflow of the project is shown in Fig. 12. Using network pharmacology dependent on the platforms specifically for the TCM, 6 and 14 core active constituents of CX and GL were identified along with 30 and 39 potential corresponding targets, respectively. The molecular docking established the PTGS2 (prostaglandin-endoperoxide synthase 2, or Cyclooxygenase-2 (COX2)) as the target with the highest binding affinity involved in both HTN and



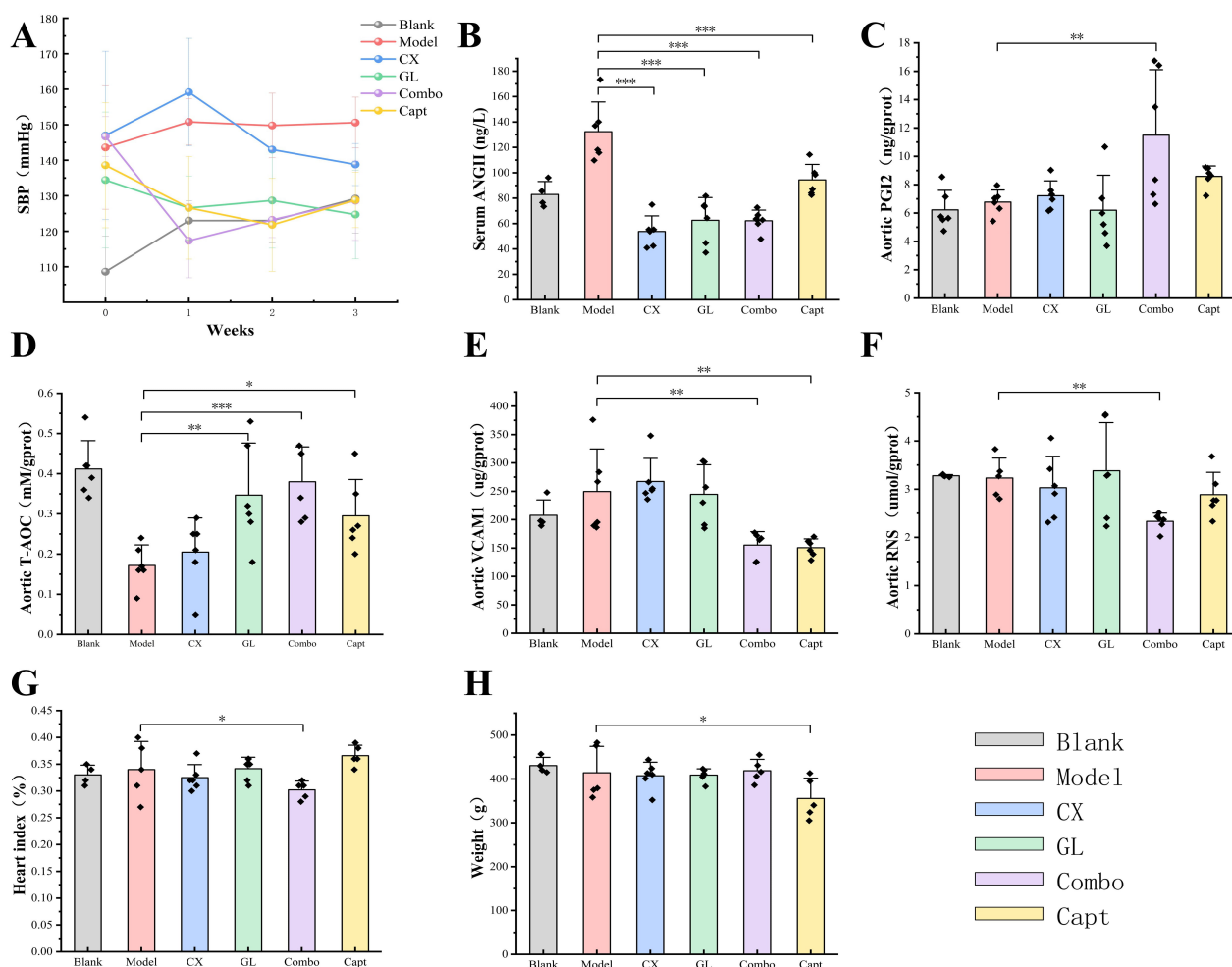


**Fig. 10. Results of indicators determination.** (A) SBP tendency during three-week administration. CI: week1 = 0.506, week2 = 0.641, week3 = 0.880. (B) Serum AngII concentration. (C) Aortic PGI2 expression. (D) Aortic T-AOC expression. (E) Aortic VCAM-1 expression. (F) Aortic RNS expression. (G) Cardiac index. (H) Body weight. Compared with the model group \* $p < 0.05$ , \*\* $p < 0.01$ , \*\*\* $p < 0.001$ .  $n = 6$ . Combo, combination of CX and GL; Capt, captopril; PGI2, prostaglandin I<sub>2</sub>; T-AOC, total antioxidant capacity; VCAM-1, vascular cell adhesion molecule-1; RNS, reactive nitrogen species.

OS for the active constituents of both CX and GL. “Estrogen signaling pathway” and “VEGF (vascular endothelial growth factor) signaling pathway” under KEGG, as well as “positive regulation of nitric oxide (NO) biosynthetic process” and “negative regulation of smooth muscle contraction” under GOBP, were significantly enriched and screened out as the mutual ones for CX and GL between the term HTN and OS, which indicated that the combination could synergistically improve vascular NO signaling conduction, smooth muscle contraction and OS induced by NO depletion involved in HTN (see Fig. 13). The following *in vivo* experimental validation suggested that, in the L-NAME induced hypertensive rat model, the combination of CX and GL contributed to significantly decreased SBP and serum ANGII, increased aortic PGI2 (the product catalyzed by PTGS2) and T-AOC, reduced aortic VCAM-1, RNS and heart index, and improved aortic damage in a synergistic way.

## 4. Discussion

TCM materials and formulas have been widely applied clinically for HTN. They not only reduce blood pressure but also broadly ameliorate pathological symptoms such as dysfunction of sympathetic system, renin-angiotensin-aldosterone system, vascular endothelium, and HTN-related risk factors, exhibiting overall regulatory characteristics [14]. As the therapeutic effects of a TCM formula derive from the interactions among multiple components and targets rather than a single one, the mechanisms of action of most TCM formulas are not easily elucidated. In our project, network pharmacology and molecular docking were employed to analyze the key components of the CX and GL combination and their corresponding mutual targets, which were then confirmed in the *in vivo* experiments, and the synergistic mechanism of the combination was effectively interpreted via the mutual signaling pathway.

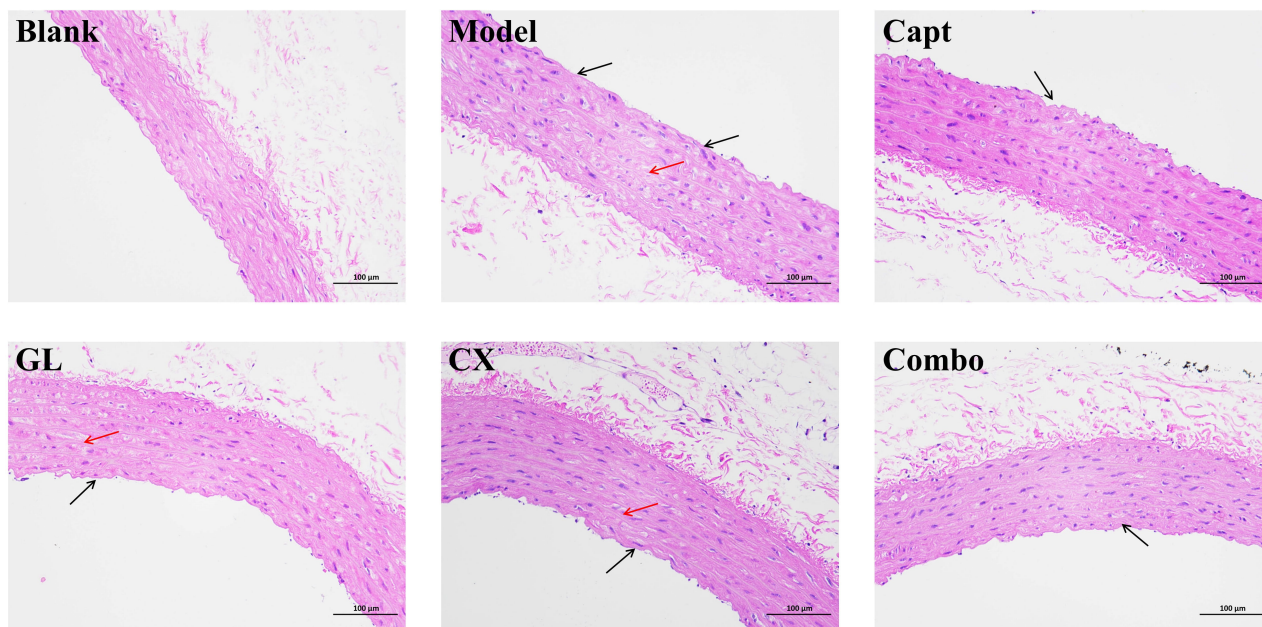


**Fig. 11. HE staining of thoracic aorta (200×).** Black arrow: deficiency of vascular endothelial structure; Red arrow: hydropic degeneration of the tunica media. *n* = 6. HE, hematoxylin-eosin staining. Scale bar = 100 μm.

Given the results of molecular docking in association with HTN and OS, respectively, the mandenol, myricanone, perlolirine, wallichilide, and FA (ferulic acid) were concluded as the core effective components for CX; the ergosta-4,6,8(14),22-tetraene-3-one, ganoderol B, lucidone A, cerevisterol and beta-sitosterol were identified as the core effective components for GL. Previous research has demonstrated that mandenol (or ethyl-linoleate) effectively reduces serum cholesterol and alleviates atherosclerotic changes in rabbits through a high-cholesterol diet [27]. Myricanone has exhibited the ability to resist oxidative damage and repair heart damage [28]. Perlolirine has been proven to alleviate pain, promote blood circulation, and exert anti-thrombotic effects [29]. Wallichilide has been found to reverse blood stasis, improve micro-circulation, and prevent focal cerebral ischemia-reperfusion injury in rats, exhibiting anti-inflammatory and anti-oxidant effects [30,31]. FA has been reported with potent antioxidant, anti-inflammatory, antibacterial, and anticancer properties [32,33]. Lucidone A has been identified with anti-oxidative and anti-inflammatory properties, preventing skin damage caused by free radicals [34]. Cerevisterol exerts anti-inflammatory effects by inhibiting inflammatory mediators and their related genes [35]. Beta-sitosterol alleviates pulmonary HTN by altering smooth muscle cell phenotype and DNA damage/cGAS/STING signaling, and effectively restores basic liver and kidney function in hypertensive rats [36,37]. Those findings suggest that the predicted active components in CX and GL demonstrate significant effects in reducing serum cholesterol for anti-oxidation, inhibiting inflammatory mediators, and improving micro-circulation and anti-thrombosis. Those effective

materials may exert a synergistic anti-hypertensive effect through multiple targets and pathways, contributing to the overall improvement of HTN. However, as the binding of the components to the targets was predicted by computational methods, their molecular interactions need to be further experimentally confirmed via Surface Plasmon Resonance (SPR), Isothermal Titration Calorimetry (ITC) or MicroScale Thermophoresis (MST), so as to clarify the mechanisms behind anti-hypertensive and vascular protective effects of CX and GL [38].

Our analysis of the core targets of active components, along with their corresponding signaling pathways and biological functions, demonstrated that the combination of CX and GL exerts multi-target effects to co-regulate multiple downstream pathways related to both HTN and OS. The mutual pathways highly associated with both HTN and OS included the “Estrogen signaling pathway” and “VEGF signaling pathway”. Studies have shown that, estrogen could regulate a plethora of physiological processes in mammals, including reproduction, cardiovascular protection, bone integrity, cellular homeostasis and behavior [39]. In the Estrogen signaling pathway for the treatment of HTN and OS, upon the activation of the estrogen receptors ESR1 and ESR2 targeted by myricanone from CX as well as OPRM1 (μ1 opioid receptor, or mu 1), JUN (Jun oncogene) and BCL2 (Apoptosis regulator Bcl-2) targeted by beta-sitosterol from GL, the downstream PGR (progesterone receptor), NCOA1 (nuclear receptor coactivator 1) and HSP90AA1 (heat shock protein 90 alpha family class A member 1) were synergistically activated through the “Nuclear-initiated steroid signaling pathway”. In turn, the triggered regulators then promoted the eNOS activity and





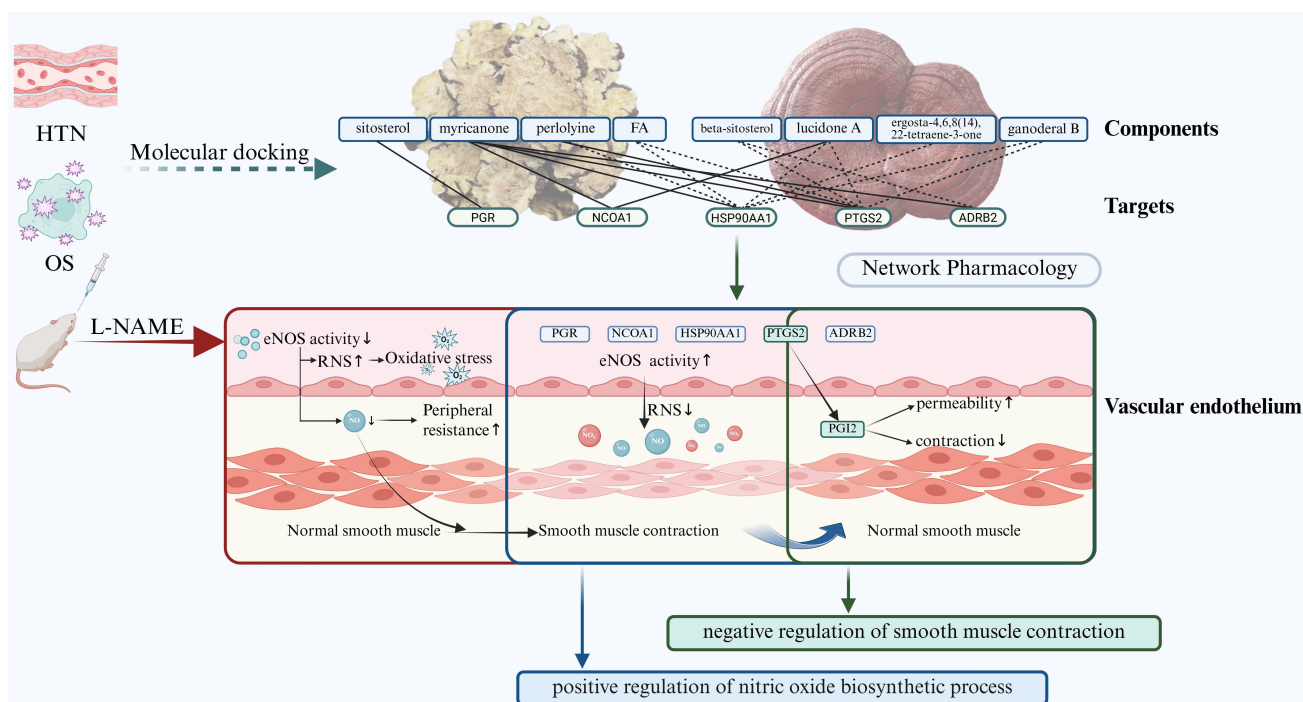


**Fig. 13. Summary of mechanism in synergistic effect of CX and GL on L-NAME induced hypertension.** Solid line between a certain target and component: experimentally validated interaction; dotted line between a certain target and component: predicted interaction. ↑: an upward trend induced by the variable; ↓: a downward trend induced by the variable. This figure was created in [BioRender.com](https://BioRender.com/aoxzk33). lu, m. (2026) <https://BioRender.com/aoxzk33>.

vascular smooth muscle relaxation [40,41], involved in the biological functions “positive regulation of NO biosynthesis” and “negative regulation of smooth muscle contraction”; typically, HTN could be regulated through the VEGF signaling pathway by promoting angiogenesis and vascular endothelial repair to improve vascular function [42,43]. In the VEGF signaling pathway related to HTN and OS, upon the activation of the VEGF receptor VEGFR2 (or KDR) and p38 (or MAPK14) targeted by myricanone from CX as well as PKC (or PRKCA) and Casp9 targeted by beta-sitosterol from GL, the downstream COX2 (or PTGS2) and ADRB2 (beta-2 adrenergic receptor) were synergistically activated. NF- $\kappa$ B is one of the most important molecules involved in inflammation [44]. The regulation of PTGS2 could improve the vascular inflammatory state through “NF- $\kappa$ B signaling pathway” [45], as evidenced by the reduced expression of aortic VCAM-1 in this study. Under conditions of increased OS, the expression and activity of COX2 altered, resulting in changes in production of various prostanoids and thus affecting vascular tone [46]. The PGI<sub>2</sub> generated by PTGS2-mediated arachidonic acid metabolism was experimentally demonstrated to significantly enhance vascular smooth muscle relaxation, functioning as a potent vasodilator in this study. ADRB2 was well known as the robust mediator for catecholamine activation of adenylate cyclase through the action of G proteins [47], which was highly associated with the regulation of vascular smooth muscle contraction. All these findings above suggest that

the combined use of CX and GL exerts complementary and synergistic anti-hypertensive effects by coordinately regulating those key signaling pathways and targets. Therefore, further experiments are necessitated. For example, expression measurement of key molecules within those pathways needs to be verified in this case, due to lack of empirical evidence regarding compatibility of CX and GL applied for treatment of HTN.

The following *in vivo* experimental results demonstrated that, the combined administration of CX and GL exhibited synergistic anti-hypertensive and anti-oxidative effects in the L-NAME induced HTN and OS model, significantly surpassing the effects of monotherapy. These effects included sustained blood pressure reduction, elevated aortic PGI<sub>2</sub> and T-AOC, reduced aortic VCAM-1 and RNS, reversal of cardiac index impairment, and vascular endothelial protection. It is noteworthy that the monotherapy of CX failed to significantly improve aortic T-AOC, whereas the combination of CX and GL exhibited a significant improvement, indicating that the vascular anti-oxidative effect was primarily mediated by GL. This finding aligns with the core therapeutic efficacy of GL as applied in TCM [48]. The results demonstrate the complementary pharmacological effects of CX and GL in the treatment of chronic OS-induced hypertension, where CX plays a dominant role in the anti-hypertensive effect. In addition, only captopril significantly reduced the body weight of participants in the model group after three-week administration ( $p < 0.05$ ), indirectly high-



lighting the safety advantages of the food-based TCM in the treatment of HTN.

This study elucidated how CX and GL exert anti-hypertensive and vascular protective effects through a network of multi-components, multi-targets and multi-pathways. The findings provide a theoretical foundation and reference for the application of CX and GL in HTN treatment. Besides, the experimentally validated active components of CX and GL involved in HTN and OS, namely, perlolyrine and FA of CX and beta-sitosterol, lucidone A, ergosta-4,6,8(14),22-tetraene-3-one and ganoderal B of GL, were predicted as the novel compounds by molecular docking in this study. A more in-depth pharmacological investigation, with particular focus on vascular endothelial effects, warrants execution for the predicted novel compounds. Such analysis would serve to more thoroughly validate the concluded mechanisms and further elucidate the medicinal value of CX and GL.

## 5. Conclusion

Leveraging the integrated approach of network pharmacology and experimental validation, this study reveals that the combined administration of *Chuanxiong Rhizoma Hort.* and *Ganoderma lucidum Karst.* synergistically alleviates L-NAME-induced hypertension. Mechanism investigations demonstrate that this herb pair co-regulates the Estrogen and VEGF signaling pathways, thereby augmenting vascular NO bioavailability, promoting vasodilation, and enhancing antioxidative defense. Those findings provide robust evidence for the therapeutic potential of this herb pair as a novel dietary-medicinal therapy for hypertension management.

## Abbreviations

L-NAME, N-Nitro-L-arginine methyl ester; CX, *Chuanxiong Rhizoma Hort.*; GL, *Ganoderma lucidum Karst.*; HTN, hypertension; OS, oxidative stress; PPI, protein-protein interaction networks; KEGG, Kyoto Encyclopedia of Genes and Genomes; GOBP, Gene Ontology biological process; SBP, systolic blood pressure; COX2, Cyclooxygenase-2; VEGF, vascular endothelial growth factor; NO, nitric oxide; ANGII, Angiotensin II human; PGI2, prostaglandin I<sub>2</sub>; PTGS2, prostaglandin-endoperoxide synthase 2; T-AOC, total antioxidant capacity; VCAM-1, Vascular Cell Adhesion Molecule-1; RNS, reactive nitrogen species; BP, blood pressure; ROS, reactive oxygen species; NOS, Nitricoxide synthase; TCM, Traditional Chinese medicine; OB, Oral bioavailability; DL, drug-likeness; GO, Gene Ontology; Combo, combination of CX and GL; Capt, captopril; CI, combination index; HE, hematoxylin-eosin staining; NBF, Neutral buffered Formalin; eNOS, endothelial Nitric Oxide Synthase; ESR1/2, Estrogen receptor1/2; VEGFR2 (KDR), Vascular Endothelial Growth Factor Receptor 2; P38 (MAPK14), mitogen-activated protein kinase;  $\mu$  (OPRM1), mu-1 opioid re-

ceptor; TF (JUN), Jun Proto-Oncogene; BCL2, Apoptosis regulator Bcl-2; PKC (PRKCA), Protein kinase C alpha type; Casp9 (CASP9), Caspase-9; CoA (NCOA1), Nuclear receptor coactivator 1; Hsp90 (HSP90AA1), Heat shock protein HSP 90-alpha; PGR, Progesterone receptor; VCAM-1, vascular cell adhesion molecule-1; FA, ferulic acid; MDA, Malondialdehyde; SOD, Superoxide dismutase; GSH, Glutathione; DNA, DeoxyriboNucleic Acid; cGAS, Cyclic GMP-AMP synthase; STING, Stimulator of interferon genes; ADRB2, Beta-2 adrenergic receptor.

## Availability of Data and Materials

All the data generated and analyzed during this study are available from the corresponding author.

## Author Contributions

ML: Writing original draft, Validation, Data curation; RW, JW, TL and JT: Validation; HL, CL, BY: Data curation, FW and JZ: Project administration, Writing original draft, Data curation, Funding acquisition. All authors contributed to editorial changes in the manuscript. All authors read and approved the final manuscript. All authors have participated sufficiently in the work and agreed to be accountable for all aspects of the work.

## Ethics Approval and Consent to Participate

The animal experiments strictly followed the 3Rs principle (Replacement, Reduction, Refinement) and the International Guiding Principles for Biomedical Research Involving Animals (CIOMS/ICLAS). All procedures complied with ethical requirements and were approved by the Experimental Animal Ethics Committee at Harbin University of Commerce (Approval No.: HSDYXY-2024066).

## Acknowledgment

Not applicable.

## Funding

The work was supported by 2024 Fundamental Research Funds in Universities of Heilongjiang Province (2024-KYYWF-1021); 2022 Harbin University of Commerce Doctoral Research Support Program (22BQ59); 2024 Heilongjiang Provincial College Student Innovation and Entrepreneurship Training Program (S202410240048).

## Conflict of Interest

The authors declare no conflict of interest.

## Supplementary Material

Supplementary material associated with this article can be found, in the online version, at <https://doi.org/10.31083/IJP46239>.

## References

- [1] Su Z, Sun JY, Gao M, Sun W, Kong X. Molecular mechanisms and potential therapeutic targets in the pathogenesis of hypertension in visceral adipose tissue induced by a high-fat diet. *Frontiers in Cardiovascular Medicine*. 2024; 11: 1380906. <https://doi.org/10.3389/fcvm.2024.1380906>.
- [2] Lachovicz R, Ferro-Lebres V, Almeida-de-Souza J. Phytotherapy: A Systematic Review for the Treatment of Hypertension. *Journal of Herbal Medicine*. 2025; 50: 100985. <https://doi.org/10.1016/j.hermed.2024.100985>.
- [3] Yang H, Xing H, Zou X, Jin M, Li Y, Xiao K, *et al.* Efficacy and safety of intensive blood pressure control in patients over 60 years: A systematic review and meta-analysis. *Clinical and Experimental Hypertension* (New York, N.Y.: 1993). 2025; 47: 2465399. <https://doi.org/10.1080/10641963.2025.2465399>.
- [4] Yang R, Zhang X, Bai J, Wang L, Wang W, Cai J. Global, regional, and national burden of hypertensive heart disease among older adults in 204 countries and territories between 1990 and 2019: a trend analysis. *Chinese Medical Journal*. 2023; 136: 2421–2430. <https://doi.org/10.1097/CM9.0000000000002863>.
- [5] Kumar V, Bishayee K, Park S, Lee U, Kim J. Oxidative stress in cerebrovascular disease and associated diseases. *Frontiers in Endocrinology*. 2023; 14: 1124419. <https://doi.org/10.3389/fendo.2023.1124419>.
- [6] Arendshorst WJ, Vendrov AE, Kumar N, Ganesh SK, Madamanchi NR. Oxidative Stress in Kidney Injury and Hypertension. *Antioxidants* (Basel, Switzerland). 2024; 13: 1454. <https://doi.org/10.3390/antiox13121454>.
- [7] Simões E Silva AC. Oxidative Stress in Renal Health. *Antioxidants* (Basel, Switzerland). 2025; 14: 144. <https://doi.org/10.3390/antiox14020144>.
- [8] Phaniendra A, Jestadi DB, Periyasamy L. Free radicals: properties, sources, targets, and their implication in various diseases. *Indian Journal of Clinical Biochemistry: IJCB*. 2015; 30: 11–26. <https://doi.org/10.1007/s12291-014-0446-0>.
- [9] Fountoulakis P, Kourampi I, Theofilis P, Marathonitis A, Papamikroulis GA, Katsarou O, *et al.* Oxidative Stress Biomarkers in Hypertension. *Current Medicinal Chemistry*. 2025. <https://doi.org/10.2174/0109298673325682241114162014>. (online ahead of print)
- [10] Tan J, Zhang J, Xie L, Sun G, Zhang X, Li P, *et al.* Influence of L-NAME-induced hypertension on spermatogenesis and sperm tsRNA profile in mice. *Biochemical and Biophysical Research Communications*. 2023; 683: 149110. <https://doi.org/10.1016/j.bbrc.2023.10.042>.
- [11] Xiong X, Wang P, Zhang Y, Li X. Effects of traditional Chinese patent medicine on essential hypertension: a systematic review. *Medicine*. 2015; 94: e442. <https://doi.org/10.1097/MD.0000000000000442>.
- [12] Gao J, Hou T. Cardiovascular disease treatment using traditional Chinese medicine: Mitochondria as the Achilles' heel. *Biomedicine & Pharmacotherapy*. 2023; 164: 114999. <https://doi.org/10.1016/j.biopha.2023.114999>.
- [13] Guo Y, Zhang R, Li W. Emodin in cardiovascular disease: The role and therapeutic potential. *Frontiers in Pharmacology*. 2022; 13: 1070567. <https://doi.org/10.3389/fphar.2022.1070567>.
- [14] Jin Z, Lan Y, Li J, Wang P, Xiong X. The role of Chinese herbal medicine in the regulation of oxidative stress in treating hypertension: from therapeutics to mechanisms. *Chinese Medicine*. 2024; 19: 150. <https://doi.org/10.1186/s13020-024-01022-9>.
- [15] Jyotirmaya SS, Rath S, Dandapat J. Redox imbalance driven epigenetic reprogramming and cardiovascular dysfunctions: phyto-compounds for prospective epidrugs. *Phytomedicine: International Journal of Phytotherapy and Phytopharmacology*. 2025; 138: 156380. <https://doi.org/10.1016/j.phymed.2025.156380>.
- [16] Wang L, Zhu X, Liu H, Sun B. Medicine and food homology substances: A review of bioactive ingredients, pharmacological effects and applications. *Food Chemistry*. 2025; 463: 141111. <https://doi.org/10.1016/j.foodchem.2024.141111>.
- [17] Zhang Y, Li D, Jia Z, Mei J, Wang Y, Zhang Y, *et al.* Zhizi-Chuanxiong herb pair alleviates atherosclerosis progression in ApoE<sup>-/-</sup> mice by promoting the methylation of FGFR3 to inhibit MAPK/ERK-mediated apoptosis. *Journal of Ethnopharmacology*. 2024; 319: 117188. <https://doi.org/10.1016/j.jep.2023.117188>.
- [18] Zhang Y, Qi Y, Jia Z, Li Y, Wu L, Zhou Q, *et al.* Effects and mechanisms of Zhizi Chuanxiong herb pair against atherosclerosis: an integration of network pharmacology, molecular docking, and experimental validation. *Chinese Medicine*. 2024; 19: 8. <https://doi.org/10.1186/s13020-023-00874-x>.
- [19] Liu SJ, Fu JJ, Liao ZY, Liu YX, He J, He LY, *et al.* Z-ligustilide alleviates atherosclerosis by reconstructing gut microbiota and sustaining gut barrier integrity through activation of cannabinoid receptor 2. *Phytomedicine: International Journal of Phytotherapy and Phytopharmacology*. 2024; 135: 156117. <https://doi.org/10.1016/j.phymed.2024.156117>.
- [20] Ren Z, Ma J, Zhang P, Luo A, Zhang S, Kong L, *et al.* The effect of ligustrazine on L-type calcium current, calcium transient and contractility in rabbit ventricular myocytes. *Journal of Ethnopharmacology*. 2012; 144: 555–561. <https://doi.org/10.1016/j.jep.2012.09.037>.
- [21] Pharmacopoeia Commission of People's Republic of China. *Pharmacopoeia of the People's Republic of China*. China Medical Science Press: Beijing. 2020.
- [22] Ahmad MF, Ahmad FA, Zeyaulah M, Alsayegh AA, Mahmood SE, AlShahrani AM, *et al.* *Ganoderma lucidum*: Novel Insight into Hepatoprotective Potential with Mechanisms of Action. *Nutrients*. 2023; 15: 1874. <https://doi.org/10.3390/nu15081874>.
- [23] Lee SY, Rhee HM. Cardiovascular effects of mycelium extract of *Ganoderma lucidum*: inhibition of sympathetic outflow as a mechanism of its hypotensive action. *Chemical & Pharmaceutical Bulletin*. 1990; 38: 1359–1364. <https://doi.org/10.1248/cpb.38.1359>.
- [24] Ru J, Li P, Wang J, Zhou W, Li B, Huang C, *et al.* TCMSP: a database of systems pharmacology for drug discovery from herbal medicines. *Journal of Cheminformatics*. 2014; 6: 13. <https://doi.org/10.1186/1758-2946-6-13>.
- [25] Fouquier J, Guedj M. Analysis of drug combinations: current methodological landscape. *Pharmacology Research & Perspectives*. 2015; 3: e00149. <https://doi.org/10.1002/prp2.149>.
- [26] Chou TC. Theoretical basis, experimental design, and computerized simulation of synergism and antagonism in drug combination studies. *Pharmacological Reviews*. 2006; 58: 621–681. <https://doi.org/10.1124/pr.58.3.10>.
- [27] Osumi Y, Amano Y, Okegawa T, Shimamoto K. Effects of ethyl-linoleate on the atheromatous changes caused by high cholesterol diet in the rabbit. *Japanese Journal of Pharmacology*. 1966; 16: 83–91. <https://doi.org/10.1254/jjp.16.83>.
- [28] Yang H, Cao J, Zhou L, Chen J, Tang J, Chen J, *et al.* Exploring the Cardioprotective Mechanisms of *Ligusticum wallichii* in Myocardial Infarction Through Network Pharmacology and Experimental Validation. *Drug Design, Development and Therapy*. 2025; 19: 281–302. <https://doi.org/10.2147/DDDT.S481499>.
- [29] Tang GH, Jiang GH, Tang XL. Effects of Chuanxiong dole and its analogues on coagulation function and hemorheology. *Chinese Pharmacological Bulletin*. 2002; 2: 238–239.
- [30] Qi H, Siu SO, Chen Y, Han Y, Chu IK, Tong Y, *et al.* Senkyunolides reduce hydrogen peroxide-induced oxidative damage in human liver HepG2 cells via induction of heme oxygenase-1. *Chemico-biological Interactions*. 2010; 183: 380–389. <https://doi.org/10.1016/j.cbi.2009.11.029>.
- [31] Wang M, Hayashi H, Horinokita I, Asada M, Iwatani Y, Liu

- JX, *et al.* Neuroprotective effects of Senkyunolide I against glutamate-induced cells death by attenuating JNK/caspase-3 activation and apoptosis. *Biomedicine & Pharmacotherapy*. 2021; 140: 111696. <https://doi.org/10.1016/j.biopha.2021.111696>.
- [32] Mancuso C, Santangelo R. Ferulic acid: pharmacological and toxicological aspects. *Food and Chemical Toxicology: an International Journal Published for the British Industrial Biological Research Association*. 2014; 65: 185–195. <https://doi.org/10.1016/j.fct.2013.12.024>.
- [33] Purushothaman JR, Rizwanullah M. Ferulic Acid: A Comprehensive Review. *Cureus*. 2024; 16: e68063. <https://doi.org/10.7759/cureus.68063>.
- [34] Kumar KJS, Yang HL, Tsai YC, Hung PC, Chang SH, Lo HW, *et al.* Lucidone protects human skin keratinocytes against free radical-induced oxidative damage and inflammation through the up-regulation of HO-1/Nrf2 antioxidant genes and down-regulation of NF- $\kappa$ B signaling pathway. *Food and Chemical Toxicology: an International Journal Published for the British Industrial Biological Research Association*. 2013; 59: 55–66. <https://doi.org/10.1016/j.fct.2013.04.055>.
- [35] Alam MB, Chowdhury NS, Sohrab MH, Rana MS, Hasan CM, Lee SH. Cerevisterol Alleviates Inflammation via Suppression of MAPK/NF- $\kappa$ B/AP-1 and Activation of the Nrf2/HO-1 Signaling Cascade. *Biomolecules*. 2020; 10: 199. <https://doi.org/10.3390/biom10020199>.
- [36] Li J, Meng ZY, Wen H, Lu CH, Qin Y, Xie YM, *et al.*  $\beta$ -sitosterol alleviates pulmonary arterial hypertension by altering smooth muscle cell phenotype and DNA damage/cGAS/STING signaling. *Phytomedicine: International Journal of Phytotherapy and Phytopharmacology*. 2024; 135: 156030. <https://doi.org/10.1016/j.phymed.2024.156030>.
- [37] Olaiya CO, Esan AM, Alabi TD. Ameliorative effects of  $\beta$ -sitosterol on some biochemical indices of hypertension in wistar albino rats. *African Journal of Medicine and Medical Sciences*. 2014; 43: 157–166.
- [38] Nowicka P, Brzeska S, Makowski M. Exploring the interactions of biologically active compounds (including drugs) with biomolecules: Utilizing Surface Plasmon Resonance and SwitchSense techniques. *TrAC Trends in Analytical Chemistry*. 2024; 176: 117764. <https://doi.org/10.1016/j.trac.2024.117764>.
- [39] Zhang D, Trudeau VL. Integration of membrane and nuclear estrogen receptor signaling. *Comparative Biochemistry and Physiology. Part A, Molecular & Integrative Physiology*. 2006; 144: 306–315. <https://doi.org/10.1016/j.cbpa.2006.01.025>.
- [40] Meyer MR, Haas E, Prossnitz ER, Barton M. Non-genomic regulation of vascular cell function and growth by estrogen. *Molecular and Cellular Endocrinology*. 2009; 308: 9–16. <https://doi.org/10.1016/j.mce.2009.03.009>.
- [41] do Nascimento GRA, Barros YVR, Wells AK, Khalil RA. Research into Specific Modulators of Vascular Sex Hormone Receptors in the Management of Postmenopausal Cardiovascular Disease. *Current Hypertension Reviews*. 2009; 5: 283–306. <https://doi.org/10.2174/157340209789587717>.
- [42] Fernández M, Semela D, Bruix J, Colle I, Pinzani M, Bosch J. Angiogenesis in liver disease. *Journal of Hepatology*. 2009; 50: 604–620. <https://doi.org/10.1016/j.jhep.2008.12.011>.
- [43] Touyz RM, Lang NN. Hypertension and Antiangiogenesis: The Janus Face of VEGF Inhibitors. *JACC. CardioOncology*. 2019; 1: 37–40. <https://doi.org/10.1016/j.jaccao.2019.08.010>.
- [44] Xu BL, Zhang GJ, Ji YB. Active components alignment of Gegenqinlian decoction protects ulcerative colitis by attenuating inflammatory and oxidative stress. *Journal of Ethnopharmacology*. 2015; 162: 253–260. <https://doi.org/10.1016/j.jep.2014.12.042>.
- [45] Kim SF, Huri DA, Snyder SH. Inducible nitric oxide synthase binds, S-nitrosylates, and activates cyclooxygenase-2. *Science (New York, N.Y.)*. 2005; 310: 1966–1970. <https://doi.org/10.1126/science.1119407>.
- [46] Zhao S, Cheng, CK, Zhang CL, Huang Y. Interplay Between Oxidative Stress, Cyclooxygenases, and Prostanoids in Cardiovascular Diseases. *Antioxidants and Redox Signaling*. 2021; 34: 784–799. <https://doi.org/10.1089/ars.2020.8105>.
- [47] Cho YY, Kim S, Kim P, Jo MJ, Park SE, Choi Y, *et al.* G-Protein-Coupled Receptor (GPCR) Signaling and Pharmacology in Metabolism: Physiology, Mechanisms, and Therapeutic Potential. *Biomolecules*. 2025; 15: 291. <https://doi.org/10.3390/biom15020291>.
- [48] Boh B, Berovic M, Zhang J, Zhi-Bin L. *Ganoderma lucidum* and its pharmaceutically active compounds. *Biotechnology Annual Review*. 2007; 13: 265–301. [https://doi.org/10.1016/S1387-2656\(07\)13010-6](https://doi.org/10.1016/S1387-2656(07)13010-6).